DESIGN AND EXPERIMENT OF ONE DIMENSION AND TWO DIMENSION METAMATERIAL STRUCTURES FOR DIRECTIVE EMISSION

Z.-B. Weng, Y.-C. Jiao, G. Zhao, and F.-S. Zhang

National Laboratory of Antenna and Microwave Technology
Xidian University
Xi'an, Shaanxi, 710071, China

Abstract—A new method to improve the gain of monopole and patch antenna with one dimension and two dimension metamaterial structures is presented. The analytical permittivity models of metamaterial are derived using the transmission line method. Then the monopole and patch antenna with the metamaterial are fabricated and measured. The experimental results show that this method is effective and these structures can realize congregating the radiation energy, thus the gain of these antennas with metamaterial increase greatly compared with the conventional ones.

1. INTRODUCTION

Metamaterials are broadly defined as artificial effectively homogeneous electromagnetic structures with unusual properties not readily available in nature. Periodic metallic structure have the ability to simulated various homogeneous material whose specific properties eventually do not exit for natural material. It has been show that a structure composed of a periodic mesh of metallic thin wires, when its characteristic dimensions are small in comparison to the wavelength, behaves as a homogenous material with a low plasma frequency [1–4]. It means that the dispersion relation of the propagating modes in this structure is shaped like in plasmas of electron gas. Several structures have been proposed to simulate metamaterials with a dielectric or magnetic plasma frequency or even both together [5–8]. This opened the field of composite materials or metamaterials for microwaves and optical applications. A special case of the metamaterial is known as a left-handed metamaterial, as under proper conditions a propagating plane wave in this media is such E, H, and k form a left handed system.

Since the idea proposed by Victor Veselago in 1968 [9], the availability of such a material is taken up nowadays and extended [10–14].

In this paper, we present a new approach for better understanding of the effective plasma frequency of metamaterial and then apply it to one dimension and two dimension antenna designs. Our aim is to find out some application of metamaterial cover in antenna through high gain design. These structures can greatly improve the gain of the monopole and patch antenna. The studies in this paper lay good foundations for the applications of metamaterial in the design of directive antennas.

2. EFFECTIVE PERMITTIVITY MODEL FROM TRANSMISSION LINE THEORY

Firstly, we will consider one kind of metamaterial: a metallic array of cylinders. As shown in Fig. 1, when the wires are lossless, the thin wire array can be described by an inductor array [6]. Here L is the wire self-inductor per unit length in Z direction. In this case, the average inductance of the array in XY plane is described by the inductance area density

$$L_s = L \cdot dx \cdot dy = \mu_0 \frac{\ln(dx/r)}{2\pi} dx dy \qquad (1)$$

On the other hand, for a plane electromagnetic wave in the vacuum, its electric field $\vec{E}$ and magnetic field $\vec{H}$ can be expressed
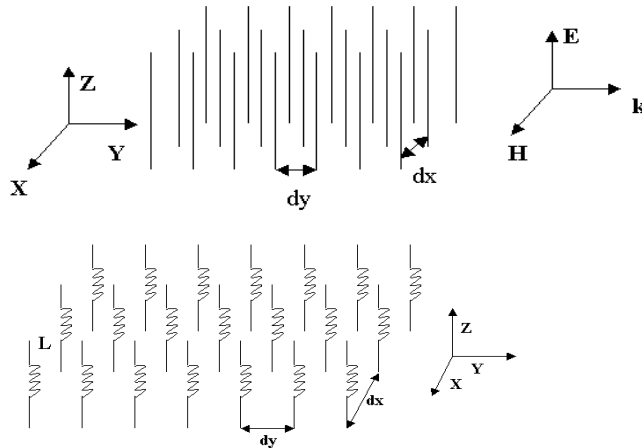

Figure 1. Inductor array equivalent to the thin wire array.

by

$$\overline{E} = \overline{\alpha}_z E_0 e^{-j\beta y}$$
$$\overline{H} = \overline{\alpha}_x H_0 e^{-j\beta y} \qquad (2)$$

Here, $\vec{\alpha}_z$ and $\vec{\alpha}_x$ are the unit vectors, β is the propagation constant in the vacuum, E_0 and H_0 are the amplitude of the $\vec{E}$ and $\vec{H}$, respectively. Obviously, it has two characters: firstly, the electromagnetic field distribution in the plane perpendicular to the direction of propagation is uniform; secondly, as shown in Fig. 2, the internal field distribution is not changed if a parallel-plate waveguide infinite in the XY plane is placed perpendicularly to the electric field direction. In this case, the plane electromagnetic wave can be represented by the internal electromagnetic wave, and the internal field can be described by the voltage $\vec{U}$ between the two plates and the surface current density $\vec{j}$ on the internal faces of the parallel-plate waveguide, respectively, as shown in Fig. 2. The $\vec{I}$ is the total current in the region d, it is given by

$$\bar{I} = d \cdot \bar{j} = d \cdot \overline{\alpha}_y \times \overline{H} = \overline{\alpha}_y d H_0 e^{-j\beta y} \qquad (3)$$

Here, d is the length of the line segment Ad. And the voltage $\vec{U}$ is given by

$$\vec{U} = h\vec{E} = \vec{\alpha}_z h E_0 e^{-j\beta y} \qquad (4)$$

Here, h is the distance between the two plates. So there is a transmission line system, it is equivalent to the free space. Based on
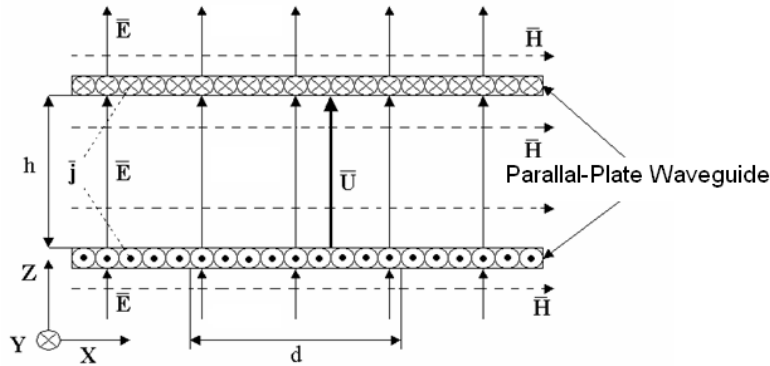

Figure 2. Equivalent field distribution in the parallel-plate waveguide.

the transmission line theory and Equations (3), (4), the characteristic
impedance is given by

$$Z = \frac{\overline{U}}{\overline{I}} = \frac{h}{d}\frac{E_0}{H_0} = \frac{h}{d}\sqrt{\frac{\mu_0}{\varepsilon_0}} = \sqrt{\frac{L_0}{C_0}} \tag{5}$$

Here, C_0 and L_0 are the distributed capacitance and inductance
per unit length of the equivalent transmission line, respectively; In
addition, the propagation constant β can be expressed by

$$\beta = \omega\sqrt{\varepsilon_0\mu_0} = \omega\sqrt{L_0C_0} \tag{6}$$

From, the equivalence between the transmission line and the free space
is derived

$$L_0 = \frac{h\mu_0}{d} \tag{7}$$

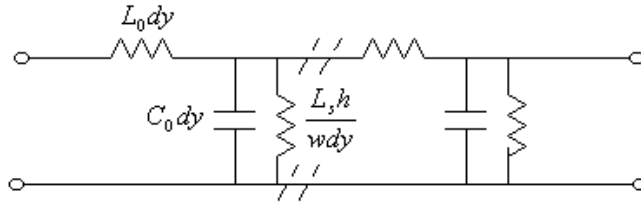$$C_0 = \frac{w\varepsilon_0}{h} \tag{8}$$

Figure 3. Equivalent circuit model of the thin wire array.

According to the above results the equivalent circuit of the thin
wire array is sketched, as shown in Fig. 3, and the circuit parameters
are related to the parameters of the array shown in (1) and the vacuum
permeability/permittivity shown in (7), (8). According to the result
the equivalent circuit of the thin wire array is sketched, as shown in
Fig. 4. In this case, the shunt inductance per unit length is expressed
as

$$L_{eq} = \frac{-1}{\omega^2 \frac{w}{h}\left(\varepsilon_0 - \frac{1}{\omega^2 L_s}\right)} \tag{9}$$

According to Caloz's LH transmission line theory

$$\begin{aligned}\varepsilon_{eff} &= -\frac{1}{\omega^2 L_{eq}\varepsilon_0} = 1 - \frac{1}{\omega^2 L_s\varepsilon_0} \\ &= 1 - \frac{2\pi/(\varepsilon_0\mu_0 dxdy\ln(dx/r))}{\omega^2} = 1 - \frac{\omega_{p1}^2}{\omega^2}\end{aligned} \tag{10}$$

Theoretical results have shown that such arrays of continuous metallic cylinders are characterized by a plasma frequency. The equivalent permittivity has a behavior governed by a plasma frequency in the microwave domain:

$$\varepsilon_{eff} = 1 - \omega_p^2/\omega^2 \tag{11}$$

where ω_p is the plasma frequency and ω is the frequency of the electromagnetic wave. The first consequence of the existence of this microwave plasma frequency is that the equivalent permittivity is negative when the frequency is below ω_p. And one other extraordinary property of such material has been less discussed: the permittivity just above the plasma frequency can be positive and less than one (still real as long as the materials are lossless). That is to say, the optical index is less than one, eventually very close to zero. Then a very low optical index is a very good candidate to design convergent micro-lenses [10].

3. DESIGN AND EXPERIMENT

3.1. 1D-periodic Metamaterial Consist of Metallic Cylinders

The first structure is metallic array of cylinders. A monopole is placed in the middle of the metamaterial and acts as the primary source. To this 1D-periodic structure, one interesting feature of this structure is its ability to generate a linearly polarized beam when the excitation current in the metallic grid flow parallel in one direction, and the electric field outside the antenna is also nearly parallel to this direction. As a consequence, the electric field outside the antenna is also nearly parallel to this direction. As mentioned above, the metamaterial can be describe by an homogeneous macroscopic material model with an effective permittivity ε_{eff}, from the expression (11) it is obvious that at low frequencies the metamaterial described by a negative permittivity, has a pure imaginary optical index. Thus the only solutions are evanescent waves. This expression also tells us that for frequencies just a little bit larger than the plasma frequency, the relative permittivity stays between 0 and 1, and the same is valid for the optical index. When the metamaterial has an effective optical index close to zero, one can expect ultra refraction phenomena.

In order to validate our approach we describe a 1-D periodic structure with this metamaterial lying on a metallic ground plane (as shown in Fig. 4). this structure is made of four layers, For easy processing and measuring, the radius of the cylinder is equal to 2 mm, the cylinder spacing d is 45 mm and $h = 120$ mm, the height and the radius of the monopole antenna is 28 mm and 0.25 mm respectively,
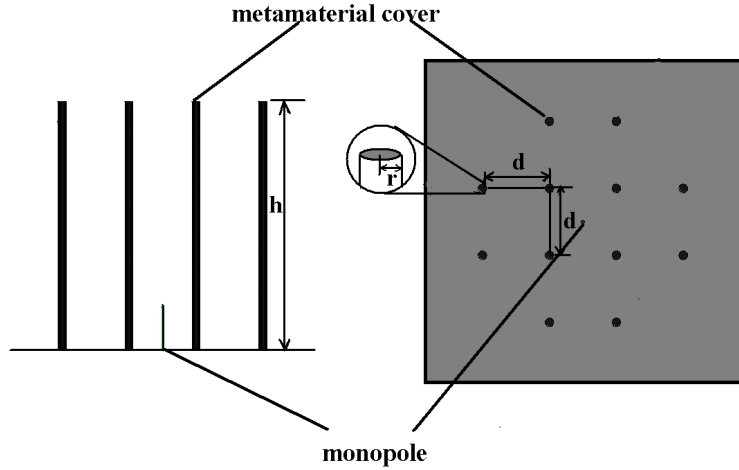
Figure 4. Schematic of the monopole system with the conformal metamaterial cover.

the size of the ground is $160 \times 160 \, \text{mm}^2$. The structure is excited with a simple monopole introduced in the middle of the metamaterial. The patterns of the monopole antenna with and without metamaterial cover have been measured in far field chamber at a distance of about $10 \, \text{m}$ (in order to be in a far field configuration). The working frequency of this antenna with cover is selected at $2.55 \, \text{GHz}$ and $2.60 \, \text{GHz}$. Since the patterns and the gain of the conventional monopole will not change too much in suitable band, we chose $2.6 \, \text{GHz}$ as its working frequency. The transmitting antenna is a ridged horn BJ22, a pyramidal horn is used as a standard antenna for measuring the gain of the monopole antenna, and the network analyzer is used for the measurements. The pattern of the monopole system has been measured in two orthogonal planes: one is the XOZ plane (the E plane) and the other is the XOY plane (the H plane). Fig. 5 shows the measured VSWR of the conventional and the metamaterial antenna. Fig. 6 shows the emission diagram in dB scales of the structure and some electrical characteristics of the antenna are shown in Table 1. As expected, since the ground is finite, the maximum is at $60 \, \text{deg}$ and $300 \, \text{deg}$ while with and without cover, the emission of the structure is concentrated in a narrow lobe in the XOZ plane and maintains its omnidirectionality in XOY plane (the un-roundness $< 3 \, \text{dB}$), since the working frequency at $2.55 \, \text{GHz}$ is closer to the plasma frequency than at $2.6 \, \text{GHz}$, the convergent property is more significant at $2.55 \, \text{GHz}$, and the gain of the monopole is increased from $5.0 \, \text{dB}$ to $7.8 \, \text{dB}$, its half power beam width is about 30 degree

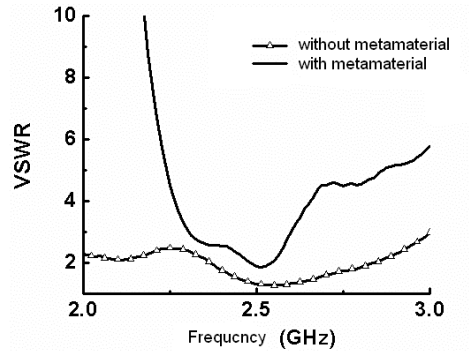**Figure 5.** Measured VSWR of the conventional monopole antenna and the metamaterial monopole antenna.

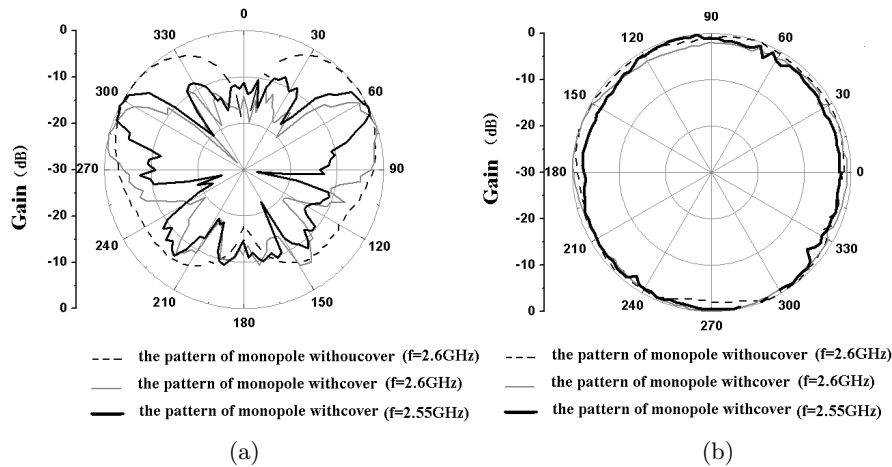(a)   (b)

Figure 6. Radiation patterns of the conventional monopole antenna and the metamaterial monopole antenna, (a) the E-plane, (b) the H-plane.

compared with the 66 degree in the conventional monopole, As an omnidirectional antenna, 2.8 dB is a great improvement in its gain.

3.2. 2D-periodic Metamaterial Consist of Modified Metallic Strips

Since the metallic strips have the similar property with the metal cylinders, a more complex 2-D structure can be realized by using a

Table 1. The electrical characteristics of the monopole with and without cover.

	frequency (GHz)	Gain (dB)	E-plane HPBW	Un-roundness
Without cover	2.60	5.0	66°	< 3 dB
With cover	2.55	7.8	30°	< 3 dB
	2.60	7.0	41°	< 3 dB

grid made of modified crossed metallic strips, which are periodically distributed in the XY plane (see Fig. 7). One function of the orthogonally directed metallic strips is to filter the cross-polarized wave components, so a source like a patch can be used in the 2-D periodic structure.
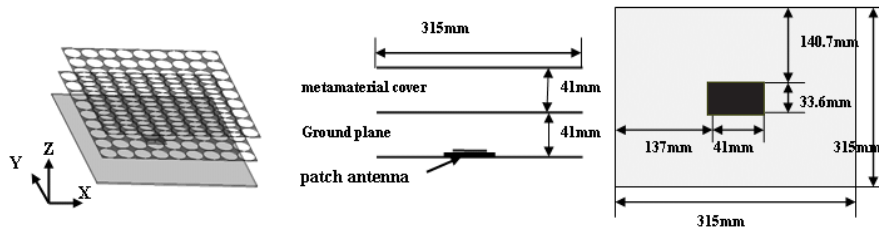
Figure 7. Patch antenna with metamaterial structure.

Based on the general antenna design process, the structure of the patch antenna is shown in Fig. 7. The patch antenna whose driven element is coaxial probe has been designed to work at 2.57 GHz. The size of the patch antenna is 41 mm×33.6 mm, The dielectric constant of the substrate is $\varepsilon_r = 2.65$, the thickness of the substrate is 1 mm, and the ground is 315 mm×315 mm. The metamaterial structure is composed of very thin copper grids with square lattices whose period a is equal to 35 mm, and the radius of ring aperture in the copper grids r is 17.2 mm. The spacing between two layers in the z-axis direction is 41 mm and each layer is composed of 9×9 cells, the total length of edge is 315 mm. The metamaterial structure is located at 41 mm from the ground.

The measured VSWR of the metamaterial patch antenna and the conventional patch antenna are shown in Fig. 8. The figure indicates that the working frequency of the patch antenna shifts slightly to
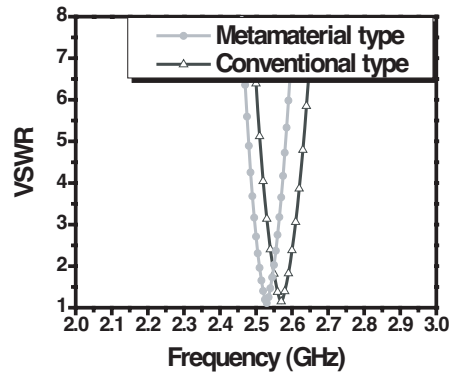
Figure 8. Measured VSWR of the conventional patch antenna and the metamaterial patch antenna.

2.53 GHz in the presence of the metamaterial cover. So the working frequency is selected at 2.55 GHz for both the conventional and the metamaterial one. The patterns of the system have been measured in two orthogonal planes: one is the x-z plane and the other is the y-z plane. Fig. 9 shows the measured radiation patterns for the conventional patch antenna and the metamaterial patch antenna in the x-z plane and the y-z plane. Some electrical characteristics of the antenna are shown in Table 2. As shown in Fig. 9, while the working frequency is chosen as 2.55 GHz, which is very close to the plasma frequency, the optical index is very close to 0and still positive, as a
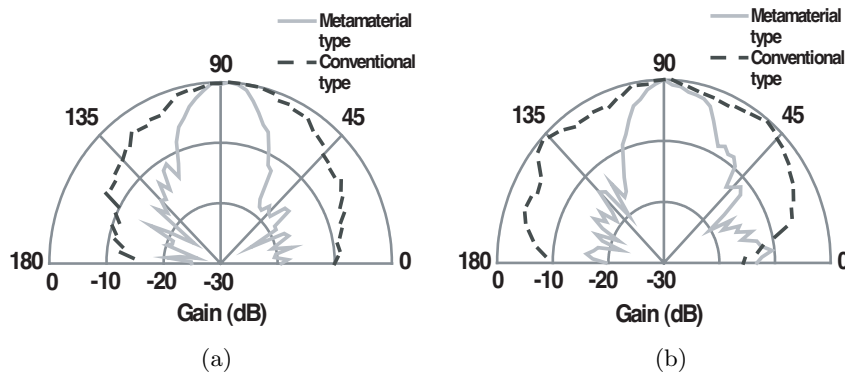

(a)   (b)

Figure 9. Measured radiation patterns for the conventional patch antenna and the metamaterial patch antenna, (a) the x-z plane, (b) the y-z plane.

Table 2. The electrical characteristics of the patch antenna with and without cover.

	Frequency (GHz)	Gain (dB)	HPBW (x-z-plane)	HPBW (y-z-plane)
Conventional type	2.55	6.8	63°	117°
Metamaterial type	2.55	17.2	25°	27°

consequence, and emission is concentrated in a narrow lobe around the normal of the structure. The measured results validate that it is effectual to raise the gain of the patch antenna by using metamaterial structure.

In theory, the maximum directivity of this antenna is $D_{\max} = 4\pi A/\lambda_0^2$, where $A = 315\,\text{mm} \times 315\,\text{mm}$, $\lambda_0 = c_0/f_0 = 117.6\,\text{mm}$, and the gain $G_{\max} = kD_{\max}$, k is the efficiency. It is assumed $k = 1$, then it is approximate to take $G_{\max}(\text{dB}) = 10\log(4\pi A/\lambda_0^2)$, so the theoretical maximum value of the antenna gain is $19.5\,\text{dB}$. The gain of the patch antenna with metamaterial structure is already very close to the theoretical maximum value of antenna with the same size and operating frequency.

4. CONCLUSION

The radiation characteristics of the monopole and patch antennas with and without metamaterial structures are measured. The measured results presented in this paper validate the concepts of our approach to control the monopole's and patch antenna's emission by using metamaterial. The radiation characteristics of antenna with metamaterial are remarkably improved. These mematerial structures are much more useful than some kinds of EBG covers in some specific applications. So our studies in this paper lay good theoretical and experimental foundations for the applications of metamaterial in antennas and other fields.

REFERENCES

1. Smith, D. R., W. J. Padilla, D. C. Vier, S. C. Nemat-Nasser, and S. Schultz, "Composite medium with simultaneously negative permeability and permittivity," *Phys. Rev. Lett.*, Vol. 84, No. 18, 4184–4187, May 2000.

2. Pendry, J. B., "Negative refraction makes a perfect lens," *Phys. Rev. Lett.*, Vol. 85, No. 18, 3966–3969, Oct. 2000.

3. Rotmant, W., "Plasma simulation by artificial dielectrics and parallel-plate media," *IRE Trans. Antennas Propagat.*, Vol. AP-10, 82–95, Jan. 1962.

4. Caloz, C. and T. Itoh, "Application of the transmission line theory of left-handed (LH) materials to the realization of a microstrip 'LH line'," *IEEE Antennas and Propagation Society International Symposium*, 412–415, Feb. 2002.

5. Smith, D. R. and N. Kroll, "Negative refractive index in left-handed materials," *Phys. Rev. Lett.*, Vol. 85, No. 14, 2933–2936, Oct. 2000.

6. Meng, F.-Y., Q. Wu, J. Wu, and L.-W. Li, "Analysis and calculation of effective permittivity for left-handed metamaterial," *Asia-Pacific Conference Proceeding*, Vol. 2, 4–7, Dec. 2005.

7. Grbic, A. and G. V. Eleftheriades, "Periodic analysis of a 2-D negative refractive index transmission line structure," *IEEE Trans. Antennas Propagat.*, Vol. 51, No. 10, 2604–2611, Oct. 2003.

8. Shelby, R. A., D. R. Smith, and S. Schultz, "Experimental verification of a negative index of refraction," *Science*, Vol. 292, 77–79, Apr. 2001.

9. Veselago, V. G., "The electrodynamics of substances with simultaneously negative values of ε and μ," *Soviet Phys. Uspekhi*, Vol. 10, No. 4, 509–514, Jan. 1968.

10. Enoch, S., G. Tayeb, P. Sabouroux, N. Guerin, and P. Vincent, "A metamaterial for directive emission," *Physical Review Letters*, Vol. 89, No. 21, 213902, 2002.

11. Li, B., B. Wu, and C.-H. Liang, "Study on hign gain circular waveguide array antenna with metamaterial structure," *Progress In Electromagnetics Research*, PIER 60, 207–219, 2006.

12. Hamid, A.-K., "Axially slotted antenna on a circular or elliptic cylinder coated with metamaterials," *Progress In Electromagnetics Research*, PIER 51, 329–341, 2005.

13. Pendry, J. B., A. J. Holden, W. J. Stewart, and I. Youngs, "Extremely low frequency plasmons in metallic microstructures," *Phys. Rev. Lett.*, Vol. 76, No. 25, 4773–4776, 1996.